

Application of Design of Experiments for Alloy Development of an Aluminum Copper Casting Alloy

Franziska Kröger and Babette Tonn

Department of Foundry Technology, Institute of Metallurgy, Clausthal University of Technology, Robert-Koch-Str. 42, Clausthal-Zellerfeld 38678, Germany

Abstract: Design of experiments (DoE) based on a linear regression model was used to develop an Aluminum Copper-based casting alloy. The main objectives of the development were the achievement of (1) a high strength at elevated temperatures with (2) a low hot tearing tendency. Within the DoE, 17 different chemical compositions of the newly developed alloy AlCuMnCo(Ni) were cast, tested regarding hot tearing tendency and characterized in tensile tests up to 300 °C. Test results showed that the AlCuMnCo(Ni)-alloys from the DoE have high mechanical properties from ambient temperature up to 300 °C and thus feature a high thermal stability. It was found that the alloying elements Cu and Co increase the yield strength whereas Mn and Ni tend to increase the attainable elongation. Furthermore, some of the alloys showed no or a very low tendency to hot tearing—a remarkable feature for Al-Cu alloys which are otherwise highly susceptible to hot tearing. The regression model that was developed from the test results fulfils a set of quality criteria and is therefore expected to provide reliable predictions. The predictive ability of the model was validated by casting and testing a sweet spot alloy. Results show that the model is sufficient for predicting the mechanical properties from ambient temperature to 250 °C. Furthermore, the sweet spot alloy surpasses the reference alloy AlCuNiCoSbZr (RR30) in its mechanical properties up to 250 °C. It was shown that by applying design of experiments, time and effort for an alloy development can effectively be reduced and simultaneously a high degree of information density about the alloying system considered is generated.

Key words: Optimization, elevated temperature properties, mechanical properties, hot tearing, AlCuMnCo(Ni).

1. Introduction

Aluminum-Copper (Al-Cu) casting alloys are precipitation hardening alloys that are well-known for their extraordinarily high strength at both ambient temperature and elevated operating temperatures. Furthermore, aluminum alloys are characterized by a high electrical and thermal conductivity and a low density of around $2.7 \text{ g}\cdot\text{cm}^{-3}$. These properties make the alloy system predestined for an application in thermally and mechanically highly loaded parts, such as cylinder heads and pistons in combustion engines or pump and bearing housings. Also, due to their high specific strength, 2xxx alloys are, beside 7xxx alloys, widely used in aircrafts [1]. Especially regarding the alloying of rare earth metals (REM) or transition

metals, there is a high potential for Al-Cu alloys for further improvement of their mechanical properties and their processability. A lot of the current research with Al-Cu focuses on alloying with rather rare and expensive elements, such as lithium (Li) or REM to push the alloy system towards very high strength (yield strength $> 450 \text{ MPa}$) [2-5]. On the other side, due to the alloys' susceptibility to hot tearing and shrinkage, research is focusing on the processability by investigating the potential of grain refinement with elements such as zirconium (Zr), scandium (Sc), vanadium (V) or cerium (Ce), by processing the alloys in semi-solid state or by applying complex processes such as rotacast® or Hero® process [6-8]. All those developments have in common that they result in either high cost materials or cost-intensive processes.

The goal of this research is to optimize an Al-Cu alloy using a maximum of four alloying elements to

Corresponding author: Franziska Kröger, M.Sc., research field: foundry technology.

both reduce the material cost and to maintain a high thermal conductivity. Furthermore, those elements are supposed to help improve the castability in gravity die casting, as one of the most inexpensive casting processes for near-net-shaped part production. Altogether, the Al-Cu alloy is supposed to feature high mechanical properties at both ambient and elevated temperatures.

2. Literature Review

2.1 Hot Tearing Tendency in Aluminum Alloys

Hot tears occur as solid-liquid failures during the solidification of metal alloys. Especially alloys with a large solidification range, such as commercially applied aluminum-zinc (Al-Zn) or aluminum-copper (Al-Cu) casting alloys, are susceptible to hot tearing whereas pure metals or eutectic alloys have no hot tearing tendency.

In principle, a lack of feeding caused by an increasingly entangled dendritic structure provokes the occurrence of casting defects like shrinkage cavities. The denser the dendritic network, the more difficult interdendritic feeding becomes and the risk of microporosity and, therefore, of hot tears increases. In addition to poor feeding characteristics, mechanical stress must be present for hot tears to form. Contraction arising during solidification of the melt might lead to stresses building up when the shrinking of the casting is restricted, as it is especially the case in permanent mold castings. Once the occurring stresses exceed the strength of the solidifying material, tears are initiated at the solid-liquid interface and may lead to a complete fracture of a cross section.

Alloys with a wide solidification range are particularly susceptible to poor feeding and hot tearing, because the fraction of solid phase increases over a long period of time and feeding gradually becomes more difficult [9]. In consequence, the chemical composition of an alloy is an important parameter to influence hot tearing, since it has an immediate influence on the width of the solidification range and

thus on the duration that the solidifying melt remains in the critical range for hot tears [10]. Furthermore, the composition mainly determines the eutectic fraction, which may decrease the hot tearing tendency with increasing fraction [11], due to its low viscosity and ability to feed a dendritic network. Also the fraction of liquid film at the end of freezing and its surface tension and wetting ability of grains is influenced by the chemical composition [12]. Besides the chemical composition, grain size and grain morphology play an important role. Several authors provided evidence that a small grain size and fine equiaxed grains improve the hot tearing resistance, due to an improved feeding capability and a more even distribution of local strains [11, 13].

Examination of the hot tearing tendency of an alloy can be done in different ways, e.g. with simple test setups like the ring test or the star mold, but also more complex *in-situ* methods, where a test mold is instrumented with displacement transducers and load cells. For this research, the star mold was used where the cast parts are optically examined for tears after casting.

2.2 Influence of Alloying Elements on Al-Cu Alloys

The technically relevant range of the Cu content in Al-Cu casting alloys is between 4.5 and 7.0 weight percent (wt%) Cu [1]. A Cu content above the maximum solubility of 5.65 wt% in aluminum leads to an improvement of high-temperature strength and to an increase in the fraction of eutectic phase Al_2Cu [14, 15]. This phase is responsible for the high attainable mechanical properties of Al-Cu alloys, especially when it precipitates from supersaturated solid solution. Up to the solubility limit, solution annealing and a subsequent quenching lead to an increase in both supersaturated solid solution with Cu and an increase in nucleation sites for Al_2Cu precipitates [16]. Above the solubility limit, excess Cu enriches the liquid phase and leads to a formation of interdendritic Al_2Cu eutectic or other Cu-containing phases [17]. Due to

the higher brittleness of interdendritic Al_2Cu compared to primary Al_2Cu precipitated from solid solution, elongation is reduced. Besides the increase in ultimate tensile strength and yield strength, an increasing Cu content causes a decrease in the solidification interval. When combined with a higher fraction of Al_2Cu eutectic, it may lead to a reduction in the hot tearing tendency of an alloy.

Literature research showed that Mn has a precipitation-hardening effect on aluminum. In the form of an intermetallic phase, Mn does not reduce the electrical conductivity as much as it does when dissolved in the α solid solution [1]. In addition, Mn shifts the formation of needle- or plate-shaped β -AlFe phases to a Chinese-script α -Al(Fe,Mn) phase when the Fe:Mn ratio is at least 5:1, better 2.5:1 [14]. In aluminum alloys Ni additions lead to an increase in strength and hardness [1, 18] and preferably form thermally stable intermetallics, e.g. the phase $\text{Al}_7\text{Cu}_4\text{Ni}$ that only starts dissolving at temperatures above 535 °C. Moreover, the formation of such intermetallics causes a reduction of Cu available for solid solution and might in consequence restrict the attainable strength [19]. Co increases both hardness and high-temperature strength [14], the latter due to a high phase precipitation temperature.

2.3 Fundamentals of Statistical Design of Experiments

Simple experimental designs are usually set up in such a way that one input variable is varied while all other input variables are kept constant in order to investigate their influence on a given output variable. Once the best result for this input variable is found, a second input variable is being varied in the same way (Fig. 1b). This procedure is called “one-factor-at-a-time” (OFAT), requires a high experimental effort, provides little information and is very inefficient. With the OFAT approach, sweet spots can only be found by chance and interactions between the input variables can not be revealed. Thus, even with a large number of experiments, the results

and correlations are only known selectively for specific variable settings.

An alternative approach is design of experiments. Design of experiments describes a methodical approach that allows to systematically uncover information and correlations within the experimental space by running only a relatively small number of experiments [20-22]. In Fig. 1a, a full factorial design is shown for three input variables, each varied on two levels. If several input variables are changed at the same time, an evaluation of the results by applying a multiple linear regression allows the isolated analysis of individual input variables as well as their interactions. By establishing a linear regression model, results are thus obtained not only at the individual variable settings but also at every point within the entire experimental space. In order to validate the model, a center point (shown in gray in Fig. 1a) is examined in two or more replicates. Thus, the variance occurring in the experiments can be assessed and an evaluation can be made regarding the quality of the model and the reproducibility of the results.

Depending on the amount of factors, the amount of experiments and the design chosen, a certain resolution of the model can be attained (s. Table 1). Depending on the resolution (III, IV or V or higher), certain effects and interactions can be explained by the model. Resolution III merely explains linear effects whereas resolution IV already allows a limited analysis of two-factor interactions, but both can not explain curvatures if they occur. Resolution V or higher allows an analysis of both linear effects and two-factor interactions, but still only in linear relationships [23]. In order to explain nonlinear behavior, designs of the response surface methodology are necessary.

A nonlinear experimental design allows the inclusion of quadratic terms. As such, e.g. Box-Behnken, Central-Composite or multiple-level full factorial designs come into consideration. In the Box-Behnken design experiments are set to the cube edges

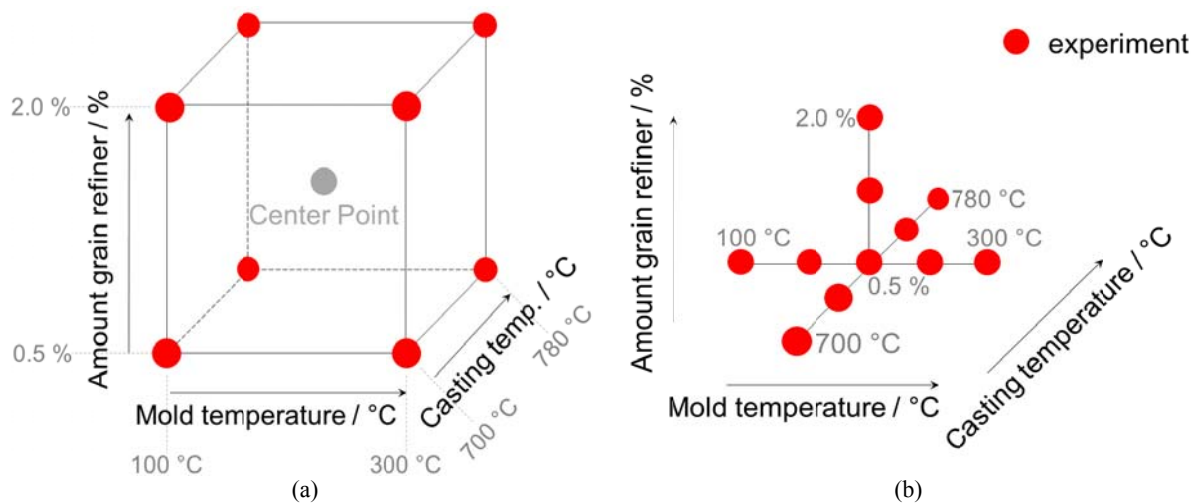


Fig. 1 Experimental design spaces with (a) design of experiments and (b) one-factor-at-a-time method.

Table 1 Resolution of designs depending on number of input variables and runs (on the basis of Ref. [23]).

		No. of input variables						
		2	3	4	5	6	7	8
No. of experiments	4	Full	III					
	8		Full	IV	III	III	III	
	16			Full	V	IV	IV	IV
	32				Full	VI	IV	IV
	64					Full	VII	V

whereas in the Central-Composite design experiments are centred above the cube surfaces [24]. If an interaction-based experimental design already exists (e.g. two-level full factorial), it can subsequently be extended with further experiments to either set up a multiple-level full factorial design or a Box-Behnken or a Central-Composite design in order to allow an inclusion of quadratic terms.

Further information and a good overview of the basics and capabilities of individual experimental designs can be found in Ref. [24]. Commercially available statistical programs for DoE are MODDE, Minitab, STATISTICA, JMP etc.

3. Application of DoE for the Development of an Al-Cu Casting Alloy

Alloy development is a complex process and usually requires many experiments to identify suitable compositional settings to achieve desired properties. For more cost and time efficiency in this process, the

DoE method is a useful tool.

For a new Al-Cu casting alloy, several properties shall be combined to meet the requirements of both foundries and their customers. The requirements comprise the following properties:

- A low hot tearing tendency to ensure the production of complex components in sand and permanent mold castings;
- A high strength that allows high loads at both ambient and elevated operating temperatures;
- A high thermal conductivity to avoid large temperature gradients and resulting thermal stresses.

For the assessment of the required properties static tensile tests up to 300 °C as well as hot tearing tests are performed. As an auxiliary parameter for the thermal conductivity serves the metallographically determined phase fraction of the as-cast material, these measurable parameters serve as quantitative output variables for the experimental design.

In preparation of the experimental design, the

objective was to identify three alloying elements that increase both mechanical properties and heat resistance and that reduce the hot tearing tendency in Al-Cu casting alloys. Therefore, benchmark tests were performed with the two commercial alloys AlCu4Ti(Mg) and AlCuNiCoSbZr in order to determine the influence of alloying elements on mechanical and hot tearing properties. The first alloy is a widely used, low-cost alloy whereas the latter alloy is an expensive alloy once developed for aircraft engines and nowadays mainly used for specific applications. In the benchmark tests, by varying the amounts of Mg, Zr, Mn and Ni in AlCu4Ti(Mg) and AlCuNiCoSbZr it is shown that in particular the elements Ni and Mn increase the high-temperature strength of the alloys. In addition, Ni leads to a slight improvement in casting properties, such as hot tearing resistance as well as flow and mold filling properties. The influence of Co was not separately tested in the benchmark tests, but there are positive results reported in literature. Therefore, as input variables the alloying elements copper (Cu), nickel (Ni), manganese (Mn) and cobalt (Co) were selected.

For this research, a two-level full factorial design with four input variables was set up, for which the four alloying elements (Cu, Ni, Mn, Co) were varied at a low and a high stage. An overview of the test parameters can be found in Table 2. The individual experiments are allocated in the corners of the design space, which is restricted by the input variables and

their levels. In order to validate the model, three experiments were carried out in the center point of the design space at a nominal composition of AlCu5.75Ni0.65Mn0.5Co0.3.

4. Experimental Work

For setting up and analyzing the design of experiments, the software MODDE (UMETRICS, Sartorius Stedim Biotech SA) was used. For the analysis of each output variable response plots are generated in order to analyze the influence of the input variables (amounts of Cu, Ni, Mn, Co) and their interactions. Thermodynamic calculations were performed with Thermo-Calc, database TCAL4. A total of 19 alloys (16 corner points and 3 center points; 12 kg each) from the DoE were melted in a medium-frequency induction furnace using Al99.8, pure Cu, AlMn26, AlCo10, AlNi20, AlTi10 and AlFe10 as raw material. The chemical composition was adjusted using optical emission spectroscopy. Fe was set to 0.1 wt% to reproduce industrial conditions. Melt treatment with a porous plug and argon gas as well as grain refinement (0.1 wt% AlTi5B1, 10 min holding time) were carried out in batches of 3.5 kg in a resistance furnace. The nominal density index to be achieved was lower than 2%. A preheated mold (300 °C) with a rod-shaped inner contour and a feeder along the entire length of the rod was used to cast the base material for the tensile test. The base material was then T7 heat-treated (see Table 3), overaged for

Table 2 Input variables, levels and output variables of the design of experiments.

Input variable alloying element	Input variable level amount in wt%	
	-	+
Cu	4.5	7.0
Ni	0.0	1.3
Mn	0.1	0.9
Co	0.1	0.5
Output variable		
UTS, YS and elongation at 23 °C, 200 °C, 250 °C and 300 °C		
Hot tearing number		
Fraction of intermetallic phases		

Table 3 Heat treatment parameters of specimens for ultimate tensile test with temperature exposure.

	Solution annealing			Quenching	Aging	Overaging
Duration in h	2	2	8	-	10	100
Temperature in °C	495	505	530	60	200	Test temp.
Medium	Air			Water	Air	Air

100 h at test temperature and then turned to B6 × 30 round tensile specimens according to DIN 50125¹. An Instron universal tensile testing machine equipped with a resistance-heated chamber furnace was used to heat up the specimens to test temperature (maximum 300 °C) for high-temperature tensile tests.

A star-shaped mold (Fig. 2), also preheated to 300 °C, was used to examine the hot tearing tendency. Each appearing crack is classified according to the crack type, evaluated accordingly (crack evaluation scheme in Fig. 2) and all crack coefficients are then summed up to a hot tearing number (HTN) which can reach a maximum of 6. The hot tearing tendency is accordingly categorized as “none” ($HTN \leq 0.5$), “low” ($0.5 < HTN \leq 1.25$), “medium” ($1.25 < HTN \leq 2.25$), “high” ($2.25 < HTN \leq 3.5$) or “very high” ($HTN \geq 3.5$).

Both alloy production and casting tests of the DoE were carried out in a randomized order.

Besides the 19 DoE-alloys, the two conventional alloys AlCu₄Ti(Mg) and AlCuNiCoSbZr (RR350) in three compositional variations (within specification limits, composition listed in Table 3 4) were cast and tested in the same manner as described above. Merely the heat treatment of specimens tested at ambient temperature differs in an additional overaging at 200 °C for 100 h.

5. Results

5.1 Model Adjustment and Analysis of the Test Results

For the experimental evaluation, all test results were added to the experimental design. Then, a model was parameterized using multiple linear regressions. To ensure a good predictability of the model, the model

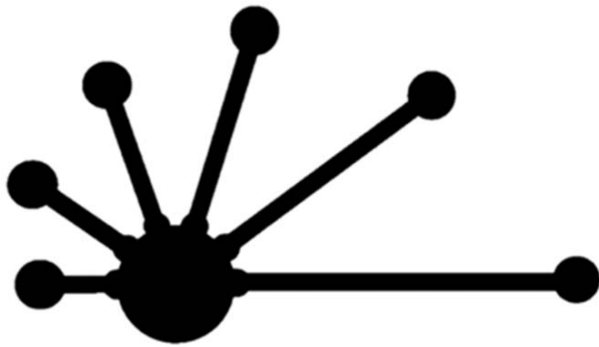
terms are adjusted in order to achieve high values of the model test parameters R^2 , Q^2 , model validity and reproducibility. R^2 as the coefficient of determination is a measure for the variance of the response that can be explained and should be higher than 0.5. Q^2 is a mathematically adapted predicted residual sum of squares (PRESS) that is converted to fit the R^2 -scale in order to make the two values comparable [25]. Q^2 stands for the predictability of the output variable and should be close to R^2 , but at least be higher than 0.5 for a good predictability. The model validity is an important value that can indicate outliers or missing model terms and should be higher than 0.25. If the model validity is lower than 0.25, the model error is higher than the pure error and there are problems with the model. The parameter reproducibility compares the deviation of the replicates with the total variation and should be higher than 0.5 [26].

The summary of fit of the model that only considers the mechanical properties is quite reliable, with R^2 ranging from 0.52 to 0.97, Q^2 from 0.32 to 0.87, model validity from 0.08 to 0.96 and reproducibility from 0.31 to 0.997. Responsible for the lowest values of R^2 and Q^2 are UTS and YS at 300 °C. Without considering the test results at 300 °C, R^2 ranges from 0.72 to 0.97, Q^2 from 0.47 to 0.87 and reproducibility from 0.57 to 0.997. The analysis of the model for the hot tearing tendency shows a low Q^2 -value of 0.016. Here, the model is probably insufficient and it is therefore expected that the predicted values will not be conform with measurements.

5.2 Analysis of Influence of Alloying Elements on Mechanical Properties and Hot Tearing Tendency of DoE Alloys

After completion of the model adjustment, an analysis of the influence of the input variables on the

¹ Test length: min. 30 mm; test diameter: 10 mm; average surface roughness: 6.3; specimen length incl. thread: min. 60 mm; height of thread: min. 8 mm; type of thread: M10.



Crack type	Appearance	Coefficient
No crack		0.0
Hairline crack		0.25
Clearly visible crack		0.5
Circumferential crack		0.75
Full crack		1.0

Fig. 2 Schematic representation of star-shaped mold for testing of hot tearing (left: downsprue in center; “bone-shaped” arms in horizontal position) and crack evaluation scheme (right).

Table 4 Chemical composition of two conventional alloys.

	Alloying elements in wt%								
	Cu	Mn	Ti	Ni	Co	Zr	Sb	Fe	Si
AlCuNiCoSbZr	4.90-5.18	0.23	0.14-0.25	1.26-1.67	0.15	0.16-0.34	0.14	0.08	0.05-0.06
AlCu ₄ Ti(Mg)	4.88-5.02	0.00-0.49	0.24-0.27	0.01-0.02	--	--	--	0.09-0.10	0.06-0.07

output variables can be carried out with the aid of so-called contour diagrams (comparable with contour lines in geographical maps). Contour plots can be created from the experimental results and allow a visual analysis of the influence of the input variables (here: alloying elements Cu, Ni, Mn and Co). A contour diagram represents the entire investigated experimental space for a selected output variable with the experiments being located on the corners of the plots. The contour lines are derived from the model and predict a value for the output variable at any point in the plot. Two such contour plots for YS and elongation at ambient temperature are shown in Figs. 3 and 4.

The analysis of the tensile tests with help of the contour diagrams makes clear that Cu causes the strongest increase in yield strength of all alloying elements. From 4.5 to 7.0 wt% Cu the yield strength rises from 120 MPa at 4.5 wt% Cu to 340 MPa at 7.0 wt% Cu, when Ni and Co are set to 1.3 wt% and 0.5 wt%, respectively, and Mn content is gradually decreased. However, an increase in Cu content leads to a reduction in the overall attainable elongation, since eutectic Al₂Cu and other Cu-containing phases precipitate from the Cu-enriched remaining melt.

Elongation is also reduced with increasing Co

content from 0.1 to 0.5 wt%. At the same time, an increase in the Co content leads to a significant increase in yield strength as can be seen in Fig. 4, the contour plot for yield strength at ambient temperature. The phase that is responsible for the increase in yield strength is probably Al₉Co₂, since, as thermodynamic calculations indicate (Table 5), its fraction increases with increasing Co content.

An EDX analysis of the as-cast material (Fig. 5 and Table 6; nominal composition AlCu4.5Mn0.1Co0.5) shows that a phase with relatively high Co content precipitated (p1 and p2) which can not be detected in the reference material with the similar composition containing 0.1 wt% Co. The morphology of the phase is textured and beaded, which is in accordance with the observations in [27], and therefore indicates that it is the phase Al₉Co₂. This phase Al₉Co₂ has similar lattice parameters as Al₃Fe (monoclinic lattice with lattice constant $b = 0.627$ nm) [27] and Fe and Cu seem to have a certain solubility in the Al₉Co₂ crystal which can be deduced from the EDX result in point p1 shown in Fig. 5 and Table 6. The phase at point p2 also has a high Co content, but seems to be a different phase than Al₉Co₂. It features a different morphology than the Al₉Co₂ phase and has a higher solubility for

Cu. Furthermore, it is embedded in a phase similar to Al_2Cu (p3 and p4 in Table 6). Possibly, it is a derivative of an $AlCuFe$ phase in which Fe atoms can be replaced by Co atoms [28]. The increase in yield

strength and decrease in elongation might therefore be a consequence of higher fractions of brittle phases like the Al_9Co_2 -phase (in accordance with Ref. [29]) that can not be dissolved in a subsequent heat treatment.

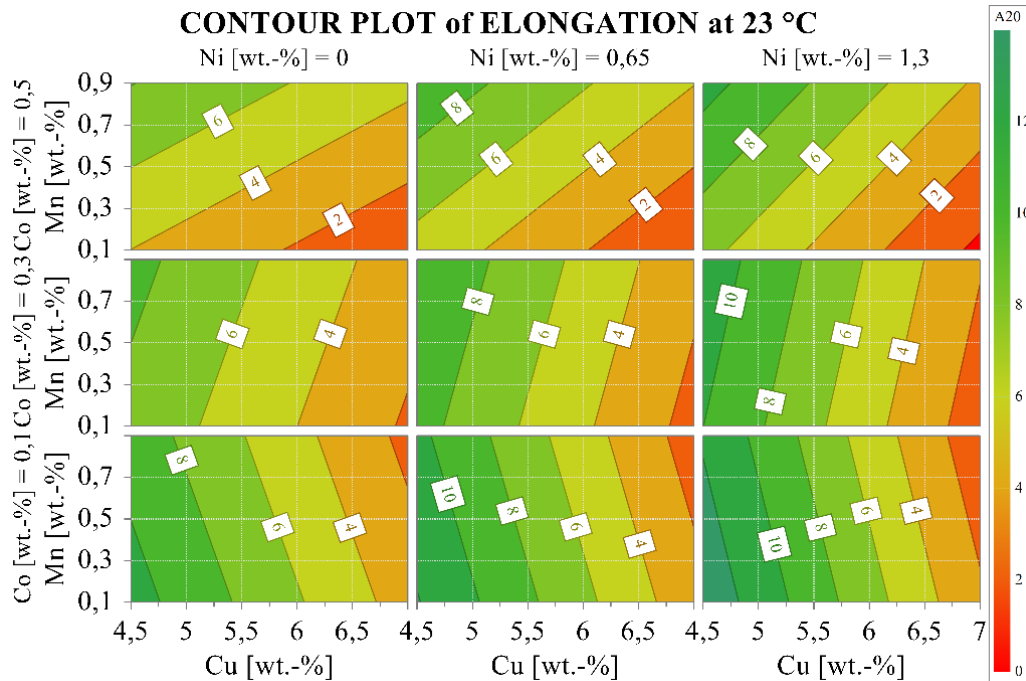


Fig. 3 Contour plot of the elongation (in %) at 23 °C test temperature with Co and Ni contents (in wt%) on the x-axis and Co and Mn contents (in wt%) on the y-axis ($R^2 = 0.85$, $Q^2 = 0.55$), MODDE 12.

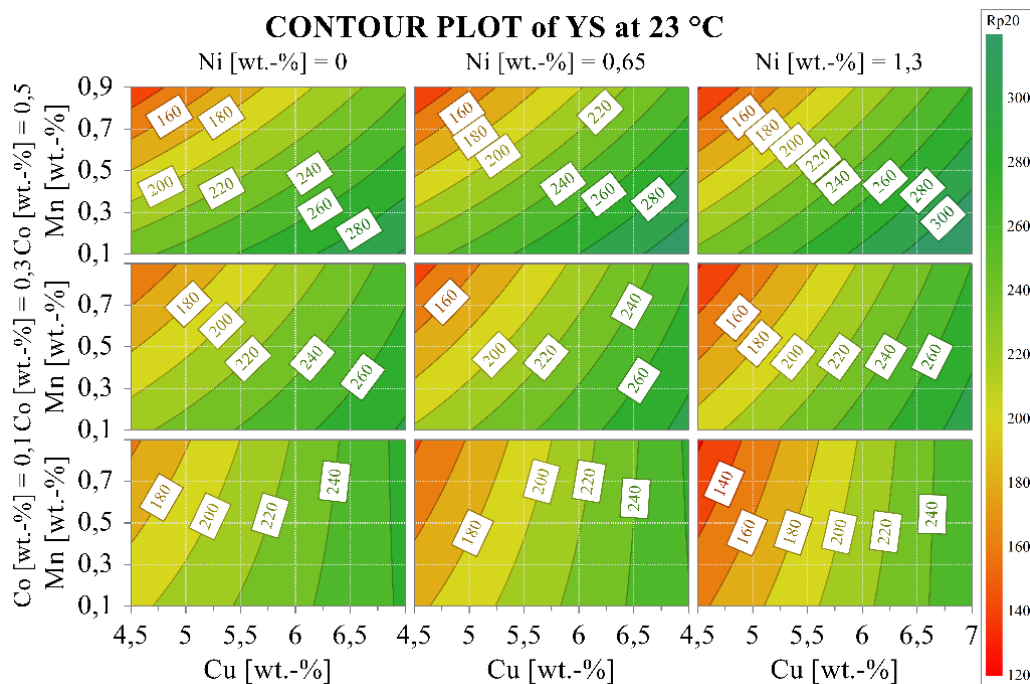
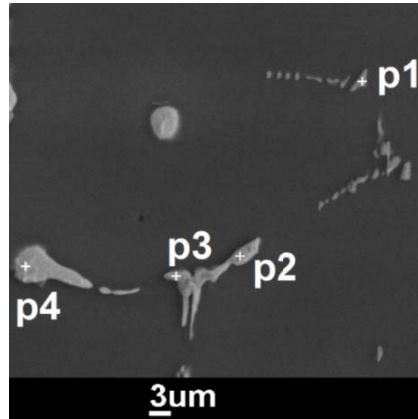


Fig. 4 Contour plot of yield strength (in MPa) at 23 °C test temperature with Co and Ni contents (in wt%) on the x-axis and Co and Mn contents (in wt%) on the y-axis ($R^2 = 0.95$, $Q^2 = 0.78$), MODDE 12.

Table 5 Phase fractions of the phases Al_9Co_2 , FCC and Al_2Cu determined in equilibrium in AlCuMnCo-alloys (Thermo-Calc, TCAL4).

Composition	Phase fraction of Al_9Co_2 in wt%	Phase fraction of FCC in wt%	Phase fraction of Al_2Cu in wt%
AlCu5Mn0.1Co0.15	0.004	0.924	0.066
AlCu8Mn0.1Co0.9	0.024	0.862	0.107
AlCu6.5Mn0.7Co0.15	0.004	0.863	0.086
AlCu6.5Mn0.7Co0.375	0.01	0.857	0.087
AlCu6.5Mn0.7Co0.9	0.024	0.843	0.087

**Fig. 5** SEM image with EDX measurements at points p1 to p4 (AlCu4.5Mn0.1Co0.5, as-cast state).**Table 6** Results of EDX measurements of point p1 to p4.

Point	Elements in at%			
	Al	Co	Cu	Fe
p1	90.5	6.7	1.5	1.0
p2	85.2	6.9	6.3	1.2
p3	89.5	0.4	10.3	0.1
p4	73.5	0.2	26.0	0.0

The contour plot in Fig. 3 also shows that at low Co contents (0.1 wt%), a combination of Co and Mn causes a reduction in elongation. Whereas, at higher Co contents, Mn compensates the detrimental effect of Co and the more Mn is added the stronger is the positive effect. With increasing contents of Mn from 0.1 (Fig. 6) to 0.9 wt% (Fig. 7), thin long Fe-containing needles, which are known to have a detrimental effect on elongation, are replaced by long Fe- and Mn-containing plate-like phases. Though, when 0.5 wt% Co is added and Mn content is low, hardly any Fe-needles but a higher content Al_9Co_2 can be seen (Fig. 8). With an increase in Mn to 0.9 wt%, the fraction of large, blocky and somewhat fissured phases increases (Fig. 9).

In contrast to the change in elongation is the change

in yield strength with increasing Mn-content (Fig. 4). Here, an increasing amount of Mn leads to a reduction of the overall attainable yield strength. This can be explained by the fact that both Cu and Mn are highly soluble in solid aluminum and might replace each other under equilibrium conditions [29, 30]. Under non-equilibrium conditions, aluminum (Al) supersaturated with Mn and Cu and non-equilibrium eutectic Al_2Cu might form during solidification (Co has a very low solubility in (Al) and can therefore be neglected here). A subsequent heat treatment above 350 °C might then lead to the formation of $Al_{20}Cu_2Mn_3$ dispersoids [30]. In consequence, this leads to a depletion of (Al) of both Cu and Mn and thereby to a reduction in overall strength.

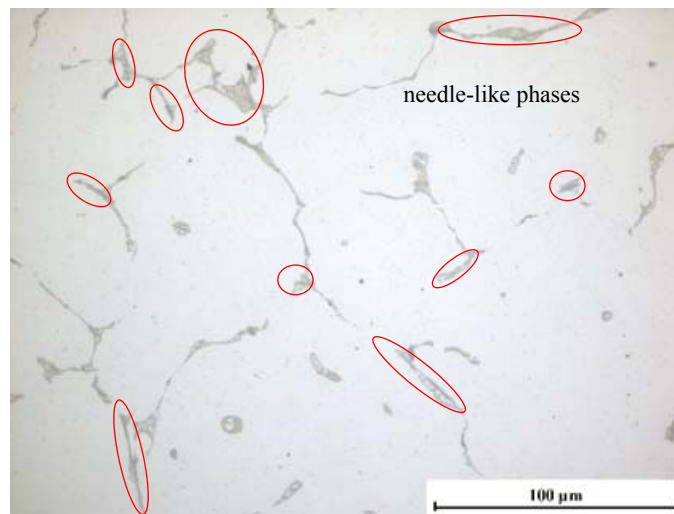


Fig. 6 Micrograph of the alloy Al_{4.5}Cu_{0.1}Mn_{0.1}Co in as-cast state with high fractions of needle-shaped phases—HTN 1.0.

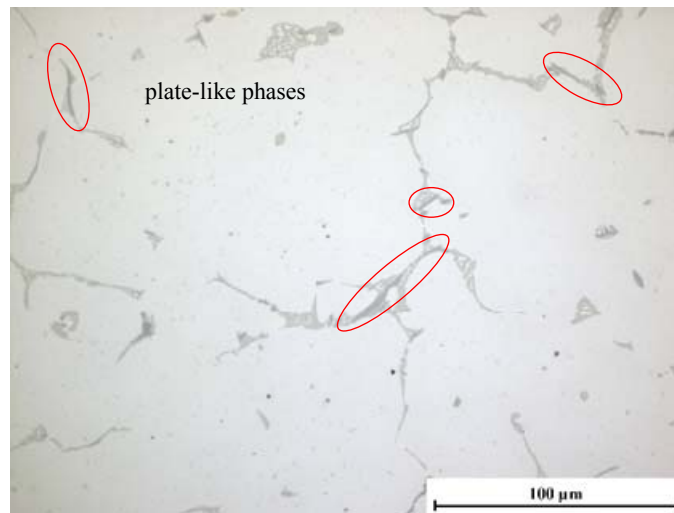


Fig. 7 Micrograph of the alloy Al_{4.5}Cu_{0.9}Mn_{0.1}Co in as-cast state containing plate-like phases—HTN 1.92.

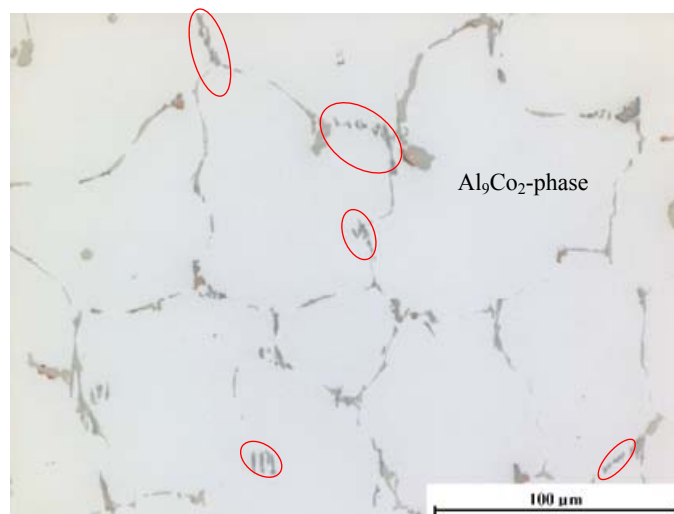


Fig. 8 Micrograph of the alloy Al_{4.5}Cu_{0.1}Mn_{0.5}Co in as-cast state with high fractions of Al₉Co₂-phase—HTN 1.4.

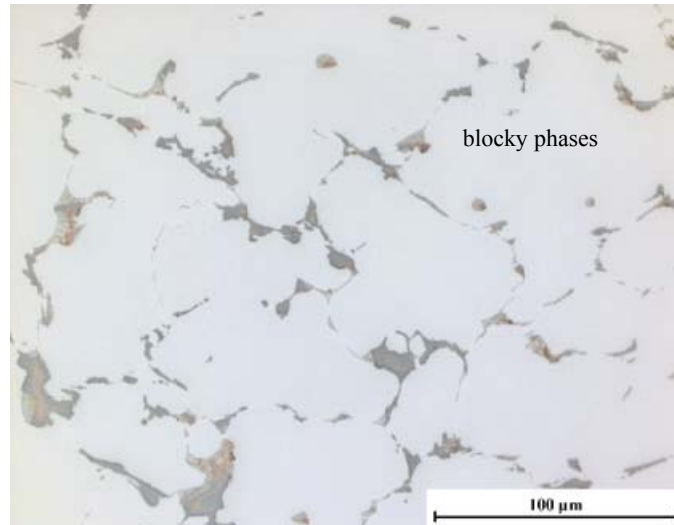


Fig. 9 Micrograph of the alloy Al_{4.5}Cu_{0.9}Mn_{0.5}Co in as-cast state with high fractions of blocky phases—HTN 2.5.

The addition of Ni leads to a significant increase in elongation (Fig. 3), especially in combination with higher Co contents, but it has hardly any effect on the yield strength (Fig. 4).

5.3 Analysis and Comparison of Commercially Available Al-Cu-Alloys and DoE-Alloys

In Figs. 10 and 11 the two mechanical properties elongation and yield strength are shown. The relationship between elongation and yield strength is reciprocally proportional. With increasing test temperature the elongation increases while the yield strength decreases. Test results that belong to the commercially available alloy AlCu₄Ti(Mg) are shown in green in Fig. 10 and results that belong to AlCuNiCoSbZr are marked in orange-yellow in Fig. 11 while in both diagrams the DoE-alloys are held in grey. To simplify reading the diagram, the test results are classified according to the test temperatures, which range from ambient temperature to 300 °C, by areas marked in grey and in color in the background.

In Fig. 10 can be seen that the AlCu₄Ti(Mg) alloy has a higher strength and higher elongation at ambient temperature than the DoE-alloys that were investigated in this research. These effects can be explained by the influence of Mg-additions to the Al-Cu system, which allow the precipitation of

hardening phases, such as Al₂CuMg and Mg₂Si. Furthermore, the copper added is predominantly available for solid solution hardening since no or merely small amounts of other elements are added that might deplete the solid solution from Cu. Even though Mg has a positive effect on the mechanical properties at ambient temperature, the element was not considered as a variable for the design of experiments in this research. Mg reduces the high temperature stability of an Al-Cu alloy due to the lower precipitation temperature of Mg-containing phases. At 300 °C test temperature, the AlCu₄Ti(Mg) alloy shows a strong decline in the yield strength with a disproportionate increase in elongation, where the DoE-alloys show much better results with an attainable yield strength of up to 105 MPa, depending on the chemical composition.

For the commercially available alloy AlCuNiCoSbZr plotting of elongation over yield strength shows that some of the DoE-alloys feature a more favorable combination of mechanical properties. Especially at room temperature, some of the DoE-alloys achieve higher yield strength values than the alloy AlCuNiCoSbZr. Overall, it can be seen that AlCuNiCoSbZr is significantly less ductile, mainly due to high amounts of alloying elements, which lead to an increase in brittle, intermetallic phase fractions.

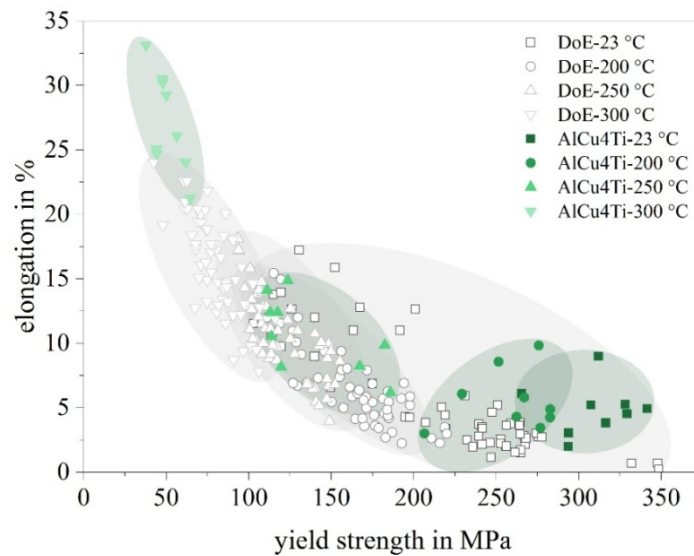


Fig. 10 Experimental results elongation and yield strength from 23 °C up to 300 °C of DoE-alloys (grey points and areas) and AlCu4Ti(Mg) alloys (green points and areas).

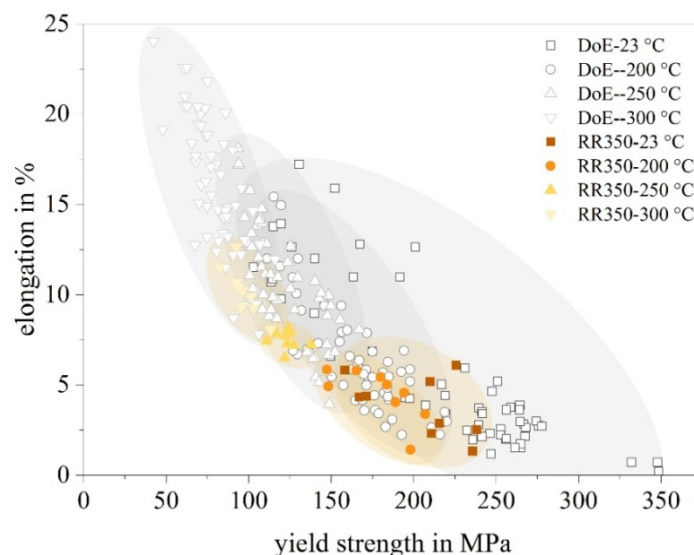


Fig. 11 Experimental results elongation and yield strength from 23 °C up to 300 °C of DoE-alloys (grey points and areas) and AlCuNiCoSbZr alloys (orange-yellow points and areas).

Besides tensile tests, all alloys were tested regarding their hot tearing tendency. All relevant experimental conditions, such as pouring and mold temperatures and the melt treatment with grain refiner additions, holding times and degassing, were kept constant. In Fig. 12 elongation is plotted once more against yield strength, this time with the mechanical properties at ambient temperature of the DoE-alloys and AlCu4Ti(Mg), categorized according to their hot

tearing tendency from “none” to “high”.

Even though the alloy AlCu4Ti(Mg) features favorable mechanical properties at ambient temperature, the hot tearing tendency of the alloy is classified as “high”. In comparison, the DoE alloys are mostly classified as alloys with “none” to “medium” hot tearing tendency and merely one composition (AlCu4.5Mn0.9Co0.5) has a high hot tearing tendency.

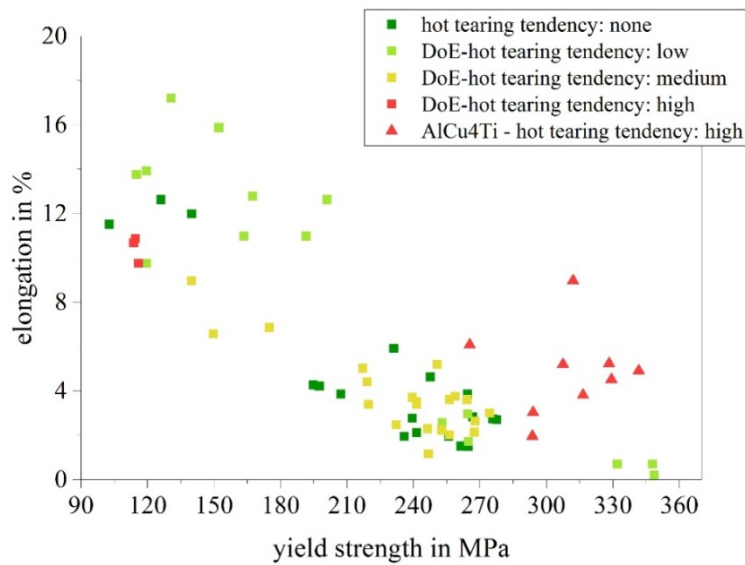


Fig. 12 Diagram of elongation over yield strength at ambient temperature with a categorization of DoE-alloys and AlCu4Ti(Mg) alloys regarding hot tearing tendency.

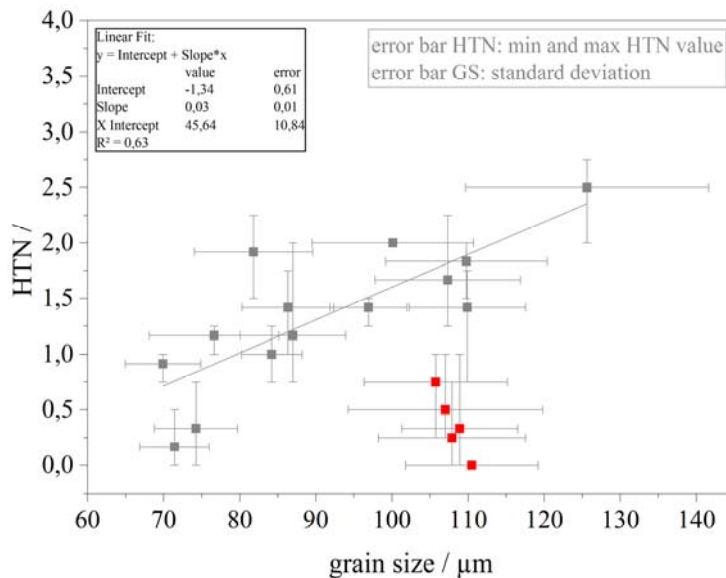


Fig. 13 Hot tearing number as a function of the grain size and linear fit without red points.

The average grain size of the DoE-alloys, determined by linear intercept method, varies between 70 and 125 μm, the grains are primarily of fine dendritic equiaxed structure and there seems to be no significant influence on the hot tearing tendency, according to the present results (Fig. 13).

An analysis of the micrographs shows that the alloys with no hot tearing tendency (HTN < 0.5, Figs. 14 and 15) have in common that most of them have a

fine eutectic on the grain boundary. Furthermore, other intermetallic phases on the grain boundaries are continuously connected in most cases and have a smooth and even interface. Coarse intermetallic phases barely appear.

In comparison, the alloy with high hot tearing tendency (2.25 < HTN ≤ 3.5, Fig. 9) has highly fragmented intermetallic phases on its grain boundaries that are unevenly spread. In some areas,

there are hardly any intermetallic phases whereas in other areas they are accumulated and coarse. There are no well-connected phases on the grain boundaries like in the alloys with no hot tearing tendency. In case films exist on the grain boundaries, they are extremely thin and rather fragmented.

The alloys with low hot tearing tendency feature smooth and even films on the grain boundaries and medium fractions of eutectic whereas the alloys with medium hot tearing tendency feature microstructural characteristics similar to the alloy with high hot tearing tendency. Intermetallic phases along the grain boundaries are fragmented and have ragged interfaces.

In summary, coarse eutectic phases seem to be disadvantageous as well as high fractions of coarse

intermetallic phases permeating eutectic since they increase an alloys' tendency to hot tearing during freezing. In contrast, smooth interfaces of phases on grain boundaries as well as high amounts of fine eutectic are favorable for a low hot tearing tendency.

5.4 Investigation of an Optimum

The application of DoE allows finding one or more sweet spots within the limits of the experimental design space that fulfill certain required properties. A useful tool for such a visual analysis is so-called sweet spot plots. For a sweet spot plot creation, (a) the desired output variables must be selected, (b) the corresponding target values must be defined and (c) the optimization direction (minimization or maximization) must be

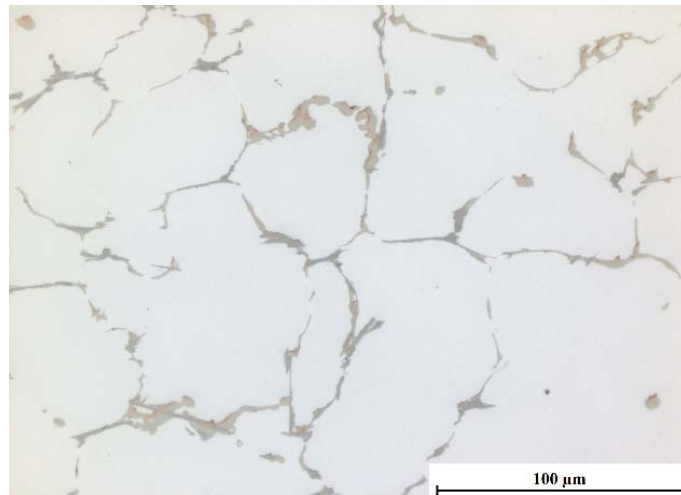


Fig. 14 Micrograph of the alloy Al7.0Cu0.1Mn0.5Co in as-cast state—HTN 0.25.

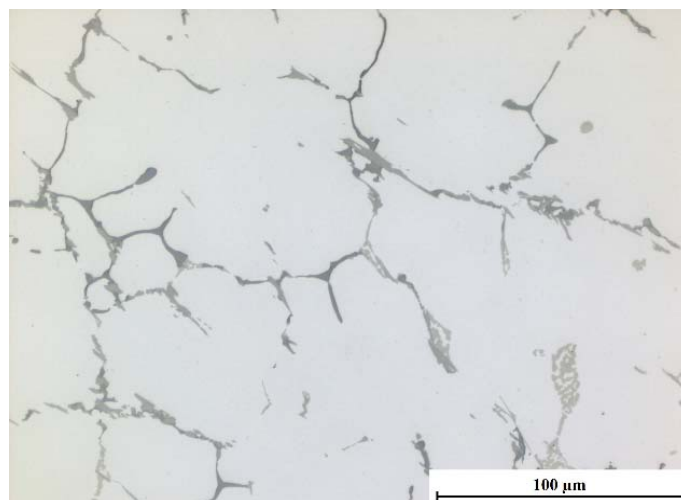


Fig. 15 Micrograph of the alloy Al5.75Cu0.5Mn0.65Ni0.3Co in as-cast state—HTN 0.22.

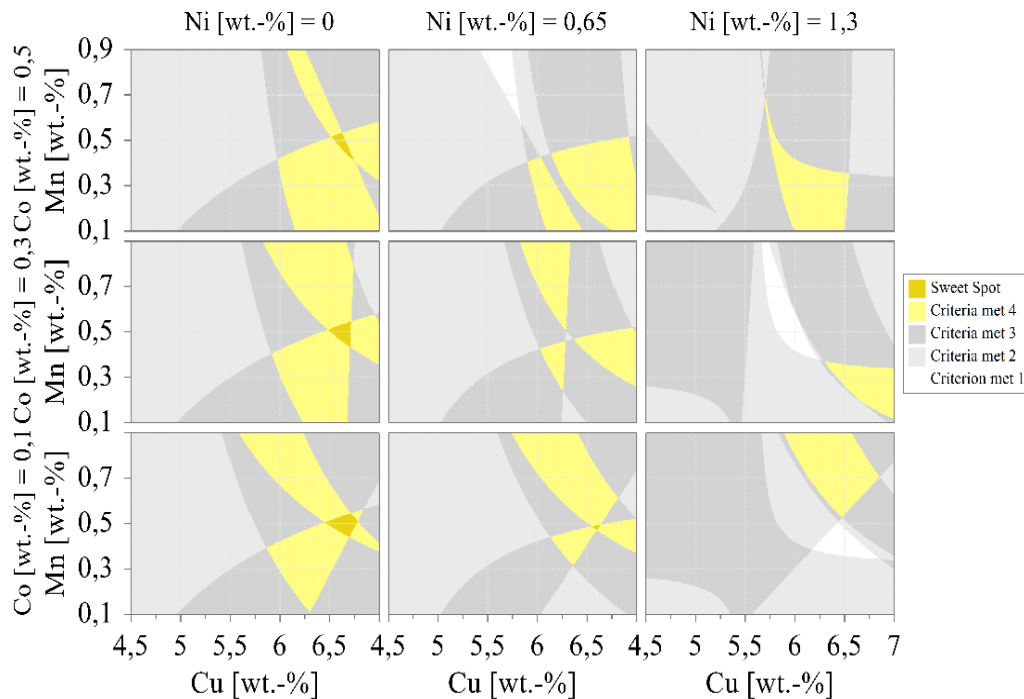


Fig. 16 Sweet spot plot of five criteria (UTS, YS and elongation at 250 °C, hot tearing tendency and phase fraction) exceeding the reference alloy AlCuNiCoSbZr.

specified. In this research an optimal chemical composition shall be found with which (a) the mechanical properties at 250 °C are (c) maximized, (a) the hot tearing tendency is (c) minimized and (a) the phase fraction is (c) minimized in order to achieve high thermal conductivity. The alloy AlCuNiCoSbZr serves as a reference, since it has high temperature properties and a comparatively low hot tearing tendency. Therefore, the best test results (mean values) of the alloys variations were used as target values for the optimization (b). By accumulation of all this information, the sweet spot plot in Fig. 16 was created.

The sweet spot plot analysis provides three chemical compositions where the requirements are fulfilled. Out of those three, the composition AlCu6.7Mn0.5Co0.1 was selected for a verification of the model predictions by testing it in experiments (casting and tensile tests). In Fig. 17 the values predicted in the model for the mechanical properties are compared to the actual measurements. With the exception of elongation at 300 °C, the predicted values are exactly met and partially exceeded, i.e. the

model predictions for the mechanical properties are correct.

When comparing the results of the sweet spot composition AlCu6.7Mn0.5Co0.1 to the alloy AlCuNiCoSbZr, up to 250 °C the mechanical properties of the “new” alloy are higher than those of the alloy AlCuNiCoSbZr. Only at 200 °C the alloy AlCuNiCoSbZr slightly exceeds the “new” alloy in its yield strength by 13%.

Regarding the hot tearing tendency, the model predicted an HTN of 0.94, which was exceeded in the experiment with an HTN of 1.58. That means that the current model does not work precisely to predict the hot tearing tendency. The aforementioned low Q^2 value already indicated such poor model quality for this output variable.

For the AlCuMnCo(Ni) alloy system investigated in this research, it was shown by testing a chemical composition in a sweet spot (AlCu6.7Mn0.5Co0.1) that the model predictions for the mechanical properties were very good, but inaccurate for the hot tearing tendency. The inaccuracy of the hot tearing prediction may be due to the experimental design

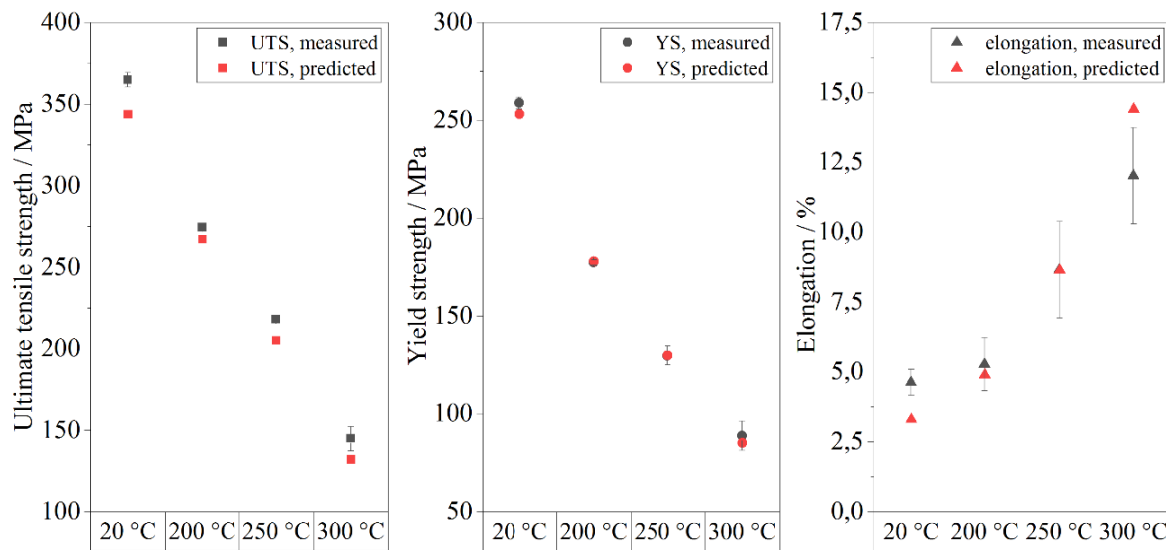


Fig. 17 Comparison of test result, predicted result and reference alloy.

itself. The DoE model showed a low predictability for the hot tearing tendency, which proved true in the subsequent test of the alloy AlCu6.7Mn0.5Co0.1, where the predicted value was not achieved. There might be two main reasons for the low predictability: on the one hand, the determination of the hot tearing tendency with the star mold is susceptible to defects due to a downward, unfiltered mold filling. This can cause turbulences and thus oxide films, which might influence the hot tearing susceptibility. On the other hand, the tendency to hot tearing may be based on a non-linear relationship with respect to the chemical composition. Other factors, such as grain refinement and microstructural properties etc., were neglected.

6. Summary

For this research, design of experiments was used to develop and optimize an Al-Cu casting alloy (a) with enhanced mechanical properties both at ambient and elevated temperatures and (b) with an improved castability by reducing the hot tearing tendency that is inherent to the Al-Cu alloy systems. Design of experiments is a well-suited tool for alloy development. With a comparatively small amount of experiments, sweet spots can be determined and valuable information about the influence of alloying

elements and interactions thereof can be obtained. In an interaction-based model, such as the two-level full factorial design used in this research, it must be taken into account that the experimental design space is set up over a chemical composition where the alloying system acts linearly. If a non-linear relationship between the input and output variables is to be expected, quadratic designs (e.g. multi-level full factorial, Box-Behnken or Central Composite designs) should be used. However, an interaction model can be expanded to a quadratic model by additional experiments where necessary.

The result is a thorough investigation of the alloy system AlCuMnCo(Ni) regarding mechanical and casting properties and the development of alloys from that alloy system with high thermal stability and a very low hot tearing tendency.

In order to investigate the influence of several alloying elements and to set benchmark values for the development, the two conventional alloys AlCu4Ti(Mg) and AlCuNiCoSbZr were tested. Within a two-level full factorial design of experiments, another 19 alloys containing copper, nickel, manganese and cobalt at different contents were cast and analyzed. The tests comprised tensile tests up to 300 °C as well as hot tearing tests.

The analysis of the tensile tests shows that an increase in copper content from 4.5 to 7.0 wt% leads to the strongest increase in yield strength compared to the other alloying elements. However, an increase in copper also leads to a reduction in elongation, since the fraction of brittle intermetallic phases in interdendritic regions increases. Cobalt also has a positive effect on the yield strength of the alloy system AlCuMnCo(Ni). At the same time, cobalt decreases the elongation if manganese contents are kept at low levels (0.1 wt%). When the manganese content is increased up to 0.9 wt%, this can lead to an improvement in elongation. However, with the increase in manganese contents, the overall attainable yield strength is reduced because of a possible depletion of (Al) of copper due to the secondary precipitation of copper- and manganese-containing phases. The addition of nickel leads, especially in combination with cobalt, to a significant increase in elongation, but has hardly any effect on the yield strength. When comparing the DoE alloys with the two commercial alloys AlCuNiCoSbZr and AlCu4Ti(Mg), it can be seen that the DoE alloys have a very good combination of yield strength and elongation from ambient to elevated temperatures and a very low hot tearing tendency, depending on the chemical composition. Whereas, though the alloy AlCu4Ti(Mg) has high mechanical properties at ambient temperature, they strongly decline up to 300 °C. Additionally, the alloy has a high tendency to hot tearing during freezing, which impairs its processability for complex castings. The alloy AlCuNiCoSbZr on the other hand, is very brittle, has low elongation and lower yield strength than the DoE alloys while the hot tearing tendency is medium. The hot tearing tests and metallographical analyses showed that a smooth interface of intermetallic phases on grain boundaries and a fine eutectic are preferable microstructural characteristics for a low hot tearing tendency in Al-Cu alloys. In contrast, rugged intermetallic phases, coarse eutectic and high amounts

of coarse intermetallic phases lead to medium to high hot tearing tendency.

Acknowledgements

The authors would like to thank the Federal Ministry for Economic Affairs and Energy (BMWi), the German Federation of Industrial Research Associations (AiF; funding No. 18647N) and the Industrial Research Association for Foundry Technology (FVG) for funding this project. Furthermore, we would like to thank our industrial partners for their support within this project and for providing materials, castings, test facilities and sharing their experience.

References

- [1] Davis, J. R., ed. 1998. *Metals Handbook*, 2nd ed. Ohio: ASM International.
- [2] Bogno, A.-A., Henein, H., and Gallermeault, M. 2018. "Design and Processing Conditions of Hypoeutectic Al-Cu-Sc Alloys for Maximum Benefit of Scandium." In *Light Metals 2018*, edited by Martin, O. Cham: Springer International Publishing, 1609-16.
- [3] Decreus, B., Deschamps, A., Geuser, F., Donnadieu, P., Sigli, C., and Weyland, M. 2013. "The Influence of Cu/Li Ratio on Precipitation in Al-Cu-Li-x Alloys." *Acta Materialia* 61 (6): 2207-18.
- [4] Rodgers, B. I., and Prangnell, P. B. 2016. "Quantification of the Influence of Increased Pre-stretching on Microstructure-Strength Relationships in the Al-Cu-Li Alloy AA2195." *Acta Materialia* 108: 55-67.
- [5] Yao, D., Bai, Z., Qiu, F., Li, Y., and Jiang, Q. 2012. "Effects of La on the Age Hardening Behavior and Precipitation Kinetics in the Cast Al-Cu Alloy." *Journal of Alloys and Compounds* 540: 154-8.
- [6] Li, J., Amhad, S., and Schumacher, P. 2019. "Grain Refinement of Al₄CuTi Based Alloy with Zr, Sc, Er and TiB₂." in *Light Metals 2019*, edited by Chesonis, C. Cham: Springer International Publishing, 1423-9.
- [7] Mathew, J., Mandal, A., Kumar, S. D., Bajpai, S., Chakraborty, M., West, G. D., and Srirangam, P. 2017. "Effect of Semi-solid Forging on Microstructure and Mechanical Properties of *In-Situ* Cast Al-Cu-TiB₂ Composites." *Journal of Alloys and Compounds* 712: 460-7.
- [8] Smetan, H. 2015. "Entwicklung serientauglicher Kokillengießverfahren für hochfeste und hochwarmfeste Al-Gusslegierungen." *GIESSEREI* 102 (3): 58-69.

- [9] Pabel, T., Bozorgi, S., Kneissl, C., Faerber, K., and Schumacher, P. 2012. "Einfluss der Legierungselemente auf die Heißrissneigung bei AlSi7MgCu-Gusslegierungen." *GIESSEREI* 99 (09): 30-7.
- [10] Katgerman, L., and Eskin, D. G. 2008. "In Search of the Prediction of Hot Cracking in Aluminium Alloys." in *Hot Cracking Phenomena in Welds II*, edited by Böllinghaus, T., Herold, H., Cross, C. E., and Lippold, J. C. Berlin, Heidelberg: Springer Berlin Heidelberg, 11-26.
- [11] Li, S., and Apelian, D. 2011. "Hot Tearing of Aluminum Alloys: A Critical Literature Review." *International Journal of Metalcasting* 5 (1): 23-40.
- [12] Sigworth, G. K. 1996. "Hot Tearing of Metals." *AFS Transactions* 155: 1053-62.
- [13] D'Elia, F., Ravindran, C., Sediako, D., Kainer, K. U., and Hort, N. 2014. "Hot Tearing Mechanisms of B206 Aluminum-Copper Alloy." *Materials & Design* 64: 44-55. doi: 10.1016/j.matdes.2014.07.024.
- [14] Kenningley, S., Koch, P., Lades, K., Morgenstern, R., Popp, M., Sobota, I., Stephan, S., Weiss, R., and Willard, R. 2014. DE 102014209102 A1. *Verfahren zur Herstellung eines Motorbauteils, Motorbauteil und Verwendung einer Aluminiumlegierung, Deutschland*.
- [15] Spittle, J. A., and Cushway, A. A. 1983. "Influences of Superheat and Grain Structure on Hot-Tearing Susceptibilities of Al-Cu Alloy Castings." *Metals Technology* 10 (1): 6-13.
- [16] Sehitoglu, H., Foglesong, T., and Maier, H. J. 2005. "Precipitate Effects on the Mechanical Behavior of Aluminum Copper Alloys: Part I. Experiments." *Metallurgical and Materials Transactions A* 36 (13): 749-61.
- [17] Kabir, M. S., Minhaj, T. I., Ashrafi, E. A., and Islam, M. M. 2014. "The Influence of Ageing Time and Temperature on the Structure and Properties of Heat Treated A201.0 Aluminum Alloy." *International Journal of Recent Technology and Engineering* 3 (3): 78-83.
- [18] Bozorgi, S., and Anders, K. 2018. "Mechanical Properties of High Copper Containing Al-Cu-Si Cast Alloys at Elevated Temperature." In *Proceedings of ICAA-16 2018*.
- [19] Hernandez-Sandoval, J., Garza-Elizondo, G. H., Samuel, A. M., Valtierra, S., and Samuel, F. H. 2014. "The Ambient and High Temperature Deformation Behavior of Al-Si-Cu-Mg Alloy with Minor Ti, Zr, Ni Additions." *Materials & Design* 58: 89-101.
- [20] Czichos, H., Saito, T., and Smith, L. 2006. *Springer Handbook of Materials Measurement Methods*. Berlin, Heidelberg: Springer Berlin Heidelberg.
- [21] Kleppmann, W. 2006. *Taschenbuch Versuchsplanung: Produkte und Prozesse Optimieren*. 4th ed., München: Hanser. <http://www.hanser-elibrary.com/isbn/9783446427747>.
- [22] Rüttimann, B. G., and Wegener, K. 2015. "The Power of DOE: How to Increase Experimental Design Success and Avoid Pitfalls." *Journal of Service Science and Management* 8 (2): 250-8.
- [23] GE Healthcare Bio-Sciences AB, ed. 2014. *Design of Experiments in Protein Production and Purification: Handbook*. Accessed Sept. 11, 2019. http://wolfson.huji.ac.il/purification/PDF/Others/GE_DOE_in_Protein_Production_and_Purification_Handbook.pdf.
- [24] Siebertz, K., Van Bebber, D., and Hochkirchen, T. 2017. *Statistische Versuchsplanung: Design of Experiments (DoE)*. 2nd ed. Berlin, Heidelberg: Vieweg. <https://ebookcentral.proquest.com/lib/gbv/detail.action?docID=5143216>.
- [25] UMETRICS. *SIMCA-P and Multivariate Analysis: Frequently Asked Questions*. Accessed Sept. 11, 2019. https://umetrics.com/sites/default/files/kb/multivariate_faq.pdf.
- [26] Sartorius Stedim Data Analytics AB, ed. 2017. *User Guide to MODDE*. Umea, Sweden. Accessed Nov. 6, 2019. <https://landing.umetrics.com/downloads-modde>.
- [27] Cheverikin, V. V., Khvan, A. V., and Zolotarevskiy, V. S. 2012. "Transforming of the Morphology of Iron Phases in Aluminum Alloys." In *Proceedings of ICAA13 Pittsburgh*, 1205-8.
- [28] Kim, S. H., Kim, B. H., Lee, S. M., Kim, W. T., and Kim, D. H. 2002. "On the Phase Transitions of the Quasicrystalline Phases in the Al-Cu-Fe-Co Alloy." *Journal of Alloys and Compounds* 342 (1-2): 246-50.
- [29] Zolotarevskij, V. S., Belov, N. A., and Glazoff, M. V. 2007. *Casting Aluminum Alloys*. Amsterdam: Elsevier. <http://site.ebrary.com/lib/alltitles/docDetail.action?docID=10188572>.
- [30] Belov, N. A., Eskin, D. G., and Aksenov, A. A. 2005. *Multicomponent Phase Diagrams: Applications for Commercial Aluminum Alloys*. Amsterdam: Elsevier. <http://site.ebrary.com/lib/alltitles/docDetail.action?docID=10138042>.